Reprinted from
PHILOSOPHICAL MAGAZINE, Vol. 11, No. 110, p. 347, February 1965

On the Structure of Coated Diamonds

By Y. KAMIYA and A. R. LANG
H. H. Wills Physics Laboratory, University of Bristol

[Received 7 September 1964]

ABSTRACT

A typical coated diamond has been examined by x-ray diffraction and absorption topography. At the commencement of the coat an abrupt change to fibrous, radial growth occurs. This radial mode of growth gives rise to the general spherical habit of thickly coated diamonds. In the specimen studied the range of misorientation in the fibrous coat was 0·43° about the fibre axis and 0·25° about a normal to the fibre axis. Fibre diameters ranged up to some tens of microns. X-ray absorption contrast produced by the more opaque layers in the coat indicated maximum local impurity concentrations of 0·7% MgO or SiO_2, or a few tenths of 1% of a heavier element such as Zr; but the concentration of Fe was less than 0·03%.

§ 1. INTRODUCTION

A typical coated diamond consists of a clear white core of good quality crystal, often a well-formed octahedron, enveloped by a green or grey coat. The material of the coat is also diamond, but is filled with dust-like matter, individual particles of which are generally of sub-micron size and are not clearly resolvable in the optical microscope. The coat has a lower specific gravity (3·50 or less) than that of pure diamond (3·515).

Cleavage persists from the core through the coat, though coat cleavage is imperfect, with matt or granular cleavage surfaces. Also, the external surface of the stone bears features, such as trigons, which have an orientation corresponding to that of the core. Thus it is evident that the orientation of coat material does not depart by more than a degree or so from that of the underlying core. The coat is usually fairly translucent, but it is not transparent. Hence coat thickness can be determined only from fracture or sectioning, or, non-destructively, by x-ray topography. In thin sections of coated stones the coat is seen to contain a number of shells of differing colour and opacity which persist as complete envelopes around the crystal.

The shape assumed by coated stones containing regular octahedral cores is a function of thickness of coat, though solution and abrasion subsequent to growth often have affected the present appearance. As the coat grows, bevels develop on edges and corners of the octahedron. The final result, with a thick coat, may be nearly a sphere. A rounded cube is an intermediate stage.

Coated diamonds are not only of considerable scientific interest but are also important commercially. More than three tons are produced

annually, most from the Congo (fraction of coated 90%), and some from Sierra Leone (up to 50% in some deposits). Stones of this type have also been reported from the new Siberian workings. The lattice texture within the coat, and the difference in lattice perfection between coat and core, are suitable matters for investigation by x-ray diffraction topography. X-ray absorption topography can also be applied to detect local concentrations of impurity. Such x-ray studies will now be reported. They have, we believe, disclosed the essential features of the structure of the coat and have thrown light upon the transition from the octahedral to the rounded habit.

Fig. 1

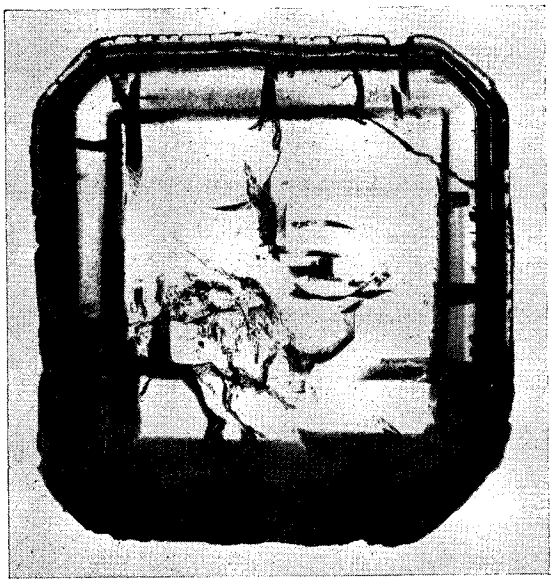

Optical transmission micrograph of plate of coated diamond. Central section parallel to a cube plane. Edges of section parallel to ⟨110⟩.

Figure 1 is an optical transmission micrograph of a section of a Sierra Leone coated stone that was chosen for study. The section is roughly parallel to a cube plane and passes close to the centre of the regular octahedron core. The diameter of the section is 5 mm, the coat thickness being about 0·8 mm. The section tapers in thickness from 0·45 mm at the bottom edge to 0·16 mm at the top: hence the variation from top to bottom in light transmission through the coat. Bands in the coat lie parallel to the octahedral boundaries of the core except at corners. Since this section makes 55° with the octahedral planes the layering of the coat is most clearly seen in the thinnest parts of the specimen. At least a dozen bands can be distinguished. Coated stones are often severely

cracked, and this stone is no exception. Cracks penetrate both coat and core. Some follow random courses, others lie in the cleavage planes. A curious occurrence in cracked coated diamonds is the partial filling of cracks with a thin film of dark material. Examples can be seen on fig. 1. Various features evident in fig. 1 will be recognized in the x-ray diffraction and absorption topographs following.

§ 2. X-ray Diffraction Topography

Projection and section topographs of various Bragg reflections have been taken with MoKα and CuKα radiations. With the latter radiation a topographic resolution of about 1 μm can be achieved. Figure 2 is a

Fig. 2

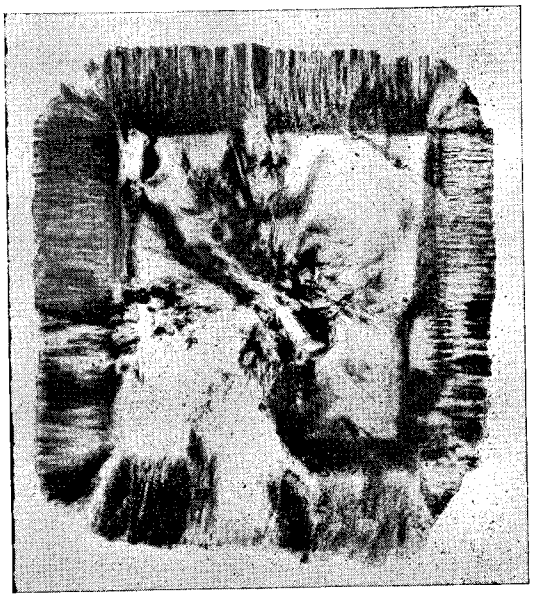

Projection topograph of plate of coated diamond. Orientation as in fig. 1, 111-type reflection.

projection topograph taken with CuKα radiation, and the same radiation was used in the other diffraction topographs reproduced here. The diffracted beam (which is always incident normally on the photographic emulsion) leaves the specimen at about 13° to the normal to the specimen surface in this 111-type reflection. Thus the geometric distortion of the image is slight and correlation between features on figs. 1 and 2 may be easily made. It is evident that a marked change in crystal texture occurs sharply at the inception of the coat. (Optical microscope studies of sections (Custers 1950) have also shown the sharpness of the core-to-coat

transition.) We will consider separately the diffraction phenomena exhibited by the core and coat, dealing first with the former.

In the core strong diffraction contrast arises from long-range strains associated with the cracks. In some parts of the core the distortion is sufficient to produce loss of reflected intensity by misorientation from the Bragg angle. (The incident beam half-width was about 100 sec of arc.) Examination of various topographs shows that a good part of the diffraction constrast arises from a strain nodulus in the centre of the specimen and from dislocation bundles which radiate from it. However, in regions remote from cracks and dislocation bundles the core behaves as a highly perfect crystal. In the upper right-hand part of fig. 2, for example, there is an area of about 1 mm square free from dislocations. Here the topograph images show only a few polishing scratches (parallel to a cube direction) and some growth stratifications parallel to octahedral planes. The latter appear more strongly in higher order reflections.

The coat, in contrast to the undistorted regions of the core, reflects with the high intensity characteristic of highly imperfect crystals. Probably most of the intensity variation seen in the image of the coat arises from varying amounts of misorientation away from the Bragg angle. These intensity variations delineate the 'fibres' or 'columns' into which the diamond becomes divided at the inception of the coat. Some banding parallel to the underlying octahedral faces of the core can be seen in the image of the coat, but it is not as well defined as in the optical micrograph. The investigation of the directions of the fibres, their cross-sectional area, and their misorientation with respect to each other and with respect to the core will now be described. However, the most important characteristic of the coat, that of radial growth, is clearly evident on fig. 2 in the way the fibres fan out at the corners of the section of the core.

Figures 3 (*a*) and (*b*) are section topographs. Figure 3 (*a*) cuts the specimen along a vertical line on fig. 2 lying to the right of the centre and fig. 3 (*b*) cuts it along a line horizontal on fig. 2 passing close to the centre. They are taken with the 220-type reflections from planes whose normals lie respectively horizontal and vertical in the plane of the specimen in the orientation of figs. 1 and 2. With these reflections the width of the image is $\sin 2\theta \sec \theta$ times the crystal thickness, i.e. 1·22 times the crystal thickness with the Bragg angle 37·7°. Thus the geometric distortion of the crystal section is not great. In both figs. 3 (*a*) and (*b*) the left-hand edge of the image is the x-ray exit surface of the specimen. Figure 3 (*a*) shows a central distorted region, rather perfect crystal above and below it, and, especially clearly in the lower, thicker part of the specimen, the sudden increase in reflecting power, and hence lattice imperfection, at the horizon where the coat begins. Figures 2 and 3 (*a*) together show that, away from edges and corners, the fibre direction is normal to the underlying octahedral surface. Figure 3 (*b*) shows generally similar features but is of interest because the top part of the section, i.e. that part cutting the

right-hand side on fig. 2, cuts through an edge of the core. Again it is seen that fibre directions fan out radially from the edge.

A measure of the misorientation in the coat was obtained by taking a series of projection topographs with the crystal angle mis-set by different amounts from the setting for peak Bragg reflection. In order to make a proper comparison between the range of misorientations about axes parallel and normal to the fibres the crystal was tilted so as to bring an octahedral plane normal to the goniometer axis and thus a set of fibres parallel to the goniometer axis. Three topographs from a series obtained

Fig. 3

(*a*) (*b*)

Section topographs, 220-type reflections. On fig. 2 the orientation of section (*a*) is vertical and (*b*) is horizontal.

this way are shown in fig. 4. They were taken with the same 220-type reflection as was used in the section topograph fig. 3 (*a*). Figure 4 (*b*) was obtained at the setting for peak reflection and figs. 4 (*a*) and (*c*) at glancing angles 0·2° smaller and greater than the peak angle, respectively. Since the difference in Bragg angles for the $K\alpha_1$ and $K\alpha_2$ radiations is 0·11° these three topographs effectively cover an orientation range of about $\frac{1}{2}$°. The range spanned by the whole series was $\frac{3}{4}$° and was sufficient to cover Bragg reflection by all parts of the crystal. The following features may be noted. The orientation spread about an axis parallel to the fibre direction exceeds that about an axis normal to the fibre direction, but not by a

Fig. 4

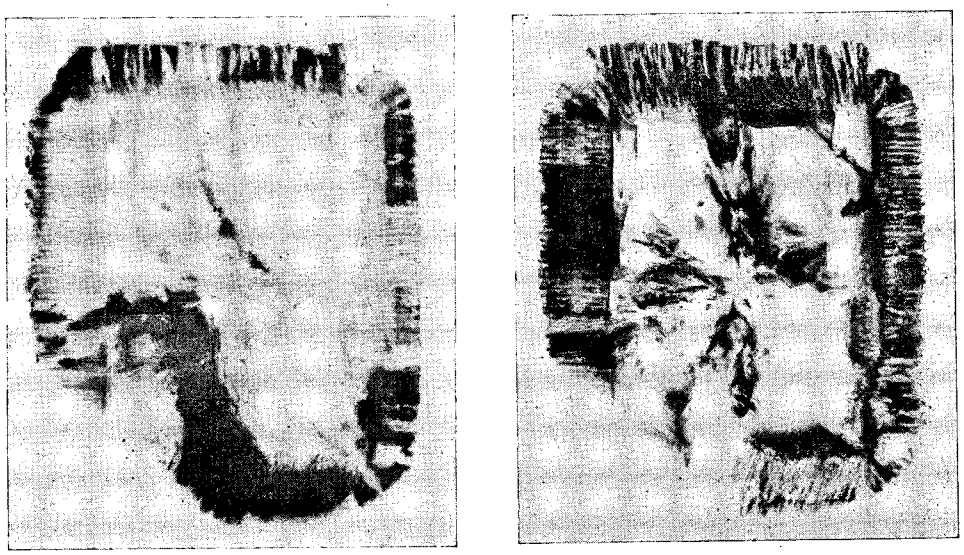

(*a*) (*b*)

(*c*)

Projection topographs showing misorientation range about vertical axis. 220-type reflection. Glancing angles, (*a*) 0·2° below peak, (*b*) at reflection peak, (*c*) 0·2° above peak. Lower left-hand corner obscured by specimen mount.

large factor. In regions not disturbed by gross misorientation of the specimen, the misorientation distribution remains fairly constant at a given horizon in the coat. Layering in the coat is shown more clearly in the off-peak topographs: jumps in the misorientation range occur at certain horizons, but not by a large factor.

More quantitative measures of misorientation were obtained by restricting the incident beam so as to cut given small sections of coat and then recording their variation of reflected intensity with glancing angle, using a scintillation counter. The values of half-widths thus obtained showed an appreciable scatter. After allowing for the Kα doublet, we obtained for the half width of the distribution of orientation with respect to rotation about the fibre direction the average value 0·43°, and, with respect to rotation about a normal to the fibre direction, 0·25°. These values refer to the coat as a whole. The increase in misorientation range going from the first layers of coat to the crystal surface was, on the average, less than 50%.

The topographs in figs. 2–4 show evidence of a coarsening of the fibre structure as the growth of coat proceeds. This feature was examined more closely by taking a set of section topographs with the incident beam cutting through the coat nearly normal to the fibre direction. This can be done with a 220-type reflection: the direct beam makes 37·7° with the reflecting plane and hence only 2·4° with an octahedral plane. In fig. 5 (*a*) the direct beam cuts the core just below the commencement of the coat. Within the coat a cellular structure is seen. Identifying the average cell size with the average fibre diameter, the following rough estimates of average diameter were obtained: at the coat commencement, 8 μm (fig. 5 *b*); after 100 μm of growth, 25 μm (fig. 5 *c*); and after another 100 μm of growth, 40 μm (fig. 5 *d*).

§ 3. X-ray Absorption Topography

Since the majority of possible impurity elements in the coat will be of greater atomic number than carbon, their presence should be detectable by microradiography with fairly soft x-rays. We have found this to be the case. There exists, moreover, the possibility of identifying the impurity, or at least of confirming the absence of certain elements in it, through the comparison of absorption topographs taken with different monochromatic radiations. Absorption topographs taken with the incident beam normal to the specimen plate revealed a series of absorbing layers corresponding in position to the more opaque bands in the coat. Their shadows were diffuse except at the thinnest part of the specimen where six absorbing layers could be resolved in a distance of 200 μm in the outer part of the coat. Since the optical and diffraction observations had shown that layers in the coat were parallel to the underlying octahedral surface of the core, a sharpening of their absorption images was obtained by tilting the plate so that the x-rays traversed it parallel to an octahedral plane. A set of absorption topographs was taken with the plate set to gain maximum